

# Thermal shock behaviour of soda lime glass.

M. Hamidouche, Z. Malou, M/A Madjoubi, C. Bousbaa, N. Bouaouadja

*Laboratoire des Matériaux Non Métalliques, Département d'O.M.P.*

*Faculté des Sciences de l'Ingénieur, Université Ferhat Abbas 19000 Sétif, Algérie*

We studied the thermal shock of a flat soda lime glass prepared with three different thickness (2 mm, 4 mm and 8 mm). We opted for descending thermal shock technique. The cooling was done by cold air jet on sample warmed beforehand. The heat transfer coefficient was about  $600 \text{ W/}^\circ\text{C.m}^2$ . The thermal shock duration was fixed to 6 seconds. The hot glass temperature was taken between  $100^\circ\text{C}$  and  $450^\circ\text{C}$  while that of the air flux was kept constant at  $20^\circ\text{C}$ .

During the exploitation of the data, we included in the computations the glass properties transient evolution with temperature. For each test, we determined the temperature profile and the transient stress states through the samples thickness. Applying the property of linear superposition of stress intensity factors, we established the evolution of the stress intensity factor  $K_I$  in function of the preexisting natural flaws in the glass. The critical flaw size was determined by the classical linear fracture mechanics laws. The critical thermal shock for each case corresponds to the point where the stress intensity factor  $K_I$  reaches the glass fracture toughness ( $K_{Ic} = 0.7 \text{ MPa.m}^{1/2}$ ). We found that as the samples thickness increases, the critical temperature decreases.

## 1- INTRODUCTION

During a sudden temperature change of a body, there occurs transient temperature gradient that induces thermal stresses. This results in a so called « thermal shock » when the body is made suddenly in contact with an environment that has a different temperature. The shock intensity is related to the temperature difference level between the initial body temperature and that of the environment. There is a distinction between an ascending thermal shock and descending one. The later one is more harmful to brittle materials as it generates tensile stresses on the rapidly cooled surface. These stresses may be sufficient to activate pre-existing micro-cracks and to lead to materials damage or fracture.

The first theoretical description was proposed by Kingery<sup>1</sup>. From a thermo-elastic analysis, he defines the critical temperature difference initiating fracture. This approach is directed towards the conditions that control the nucleation of fracture. Another approach that treats the propagation rather than the nucleation of cracks is that of Hasselman<sup>2</sup>. His theory enables to characterise the critical temperature difference as well as the damage degree of the materials. It takes into consideration the pre-existing cracks instability in relation with the temperature difference.

Manson<sup>3</sup> introduced the Weibull distribution in the case of thermal shock. He showed that the surface stress level is higher than the expected values for high probability of fracture. Another more realistic approach known as the local approach in comparison with the preceding global approaches was proposed by Evans<sup>4</sup> and completed by Schneider<sup>5</sup>. This fine analysis enables to treat the processes occurring during the thermal shock. It takes into account the transitory character of the thermal shock by determining at every instant the temperature profile, the corresponding stress state and the stress intensity factor in relation with the crack size.

Experimental methods for controlling thermal shock damage are numerous. There are static methods for measuring the material scaling, the weight loss and the mechanical strength deterioration. Other dynamic methods permit to control the damage by measuring the frequency disturbances and the stationary or moving waves damping caused by the thermal shock.

## 2- EXPERIMENTAL PROCEDURE

The glass used in this study is a silica soda lime glass made by ENAVA company (Algeria). Its chemical composition contains mainly 71.56 % of SiO<sub>2</sub>, 13.73% of Na<sub>2</sub> O, 7.91 % of CaO, 4 % MgO, 1.9 % Al<sub>2</sub>O<sub>3</sub> and 0.2 % impurities. The main characteristics of the tested material, measured at ambient temperature, are gathered in table 1.

Table 1: Some physical characteristics of ENAVA glass

Physical properties	property value	experimental technique used
Poisson coefficient $\nu$	0.22	ultrasonic wave
Density $\rho$	2.52 g/cm <sup>3</sup>	Archimedes method
Fracture toughness K <sub>1c</sub>	0.75 MPa m <sup>1/2</sup>	S.E.N.B.
Hardness Hv	4.7 GPa	Vickers
Mechanical strength $\sigma_r$	82 MPa	3 point-bending
Transient temperature T <sub>g</sub>	524 °C	Differential Thermal Analysis

Some glass properties in function of temperature were measured. To study the dilatometric behaviour, a test was carried out from ambient temperature to 500 °C on a silica sample holder dilatometer. The thermal expansion curve versus temperature can be fitted by this equation:

$$\alpha(T) = 9.10^{-9} + 2.10^{-9} T \quad [^{\circ}\text{C}^{-1}] \quad (1)$$

The Young's modulus E was measured as a function of temperature by the resonance frequency in bending with a grindo sonic apparatus:

$$E(T) = 72 - 6.61 T - 0.016 T^2 - 10^{-5} T^3 \quad [\text{GPa}] \quad (2)$$

The thermal conductivity was derived from the literature <sup>6</sup>. In the range from 20 to 600 °C, it can be fitted by:

$$K = 1.576 - 9.10^{-4} T + 3.10^{-6} T^2 \quad [\text{W/m/}^{\circ}\text{C}] \quad (3)$$

The specific heat Cp was also derived from the literature <sup>6</sup> since it is mostly dependent on the chemical composition:

$$C_p = 217.7 + 1.01 T - 3.10^{-4} T^2 \quad [\text{J/kg/}^{\circ}\text{C}] \quad (4)$$

Since the Poisson's ration is generally weakly dependent on the temperature, it was only measured at room temperature by the wave velocity method:  $\nu = 0.22$

The test was made using a descendant thermal shock test type. The sample is maintained at hot temperature during six minutes for making the temperature uniform. The sample transportation to the cold zone takes approximately three seconds. The cooling process lasts 6 s. Strength measurements were made after the thermal shock tests using a four point bending configuration with an inner and an outer span of respectively 10 and 35 mm. The tests were carried out in air using an Instron testing machine. The crosshead speed was 0.5 mm/min.

The modelisation is based on local approach of the thermal shock. The model used is in two directions (2D) cross section of a rectangular beam was modelled. Because of symmetry, we concentrated on one sample quarter. We began by determining the transitory temperature distribution. We then evaluate the transient superficial stresses and finally the

stress intensity factor using the superposition principle of. We integrated in this numerical procedure the temperature dependence of the glass thermo-elastic properties. It is important to point out that the frontal and lateral heat transfer are identical and remain independent of temperature ( $h = h_f = h_l = 600 \text{ W}/(\text{m}^2 \cdot ^\circ\text{C})$ ). It enables to evaluate bidimensionnally the temperatures and the stresses at every instant of the thermal shock and at every point on the sample.

We were especially interested to fracture initiation moments during the cooling process and to the crack initiation site (near the centre of the  $40 \times 2 \text{ mm}^2$ ,  $40 \times 4 \text{ mm}^2$  or  $40 \times 8 \text{ mm}^2$  sample surfaces).

## 2- RESULTS AND DISCUSSION

First of all, we determined the temperature difference ( $T_c - T_s$ ) between the sample inner center ( $x=l/2$ ) and its surface ( $x=0$ ) in function of the cooling duration for different imposed temperature gradient  $\Delta T$  on the glass with three different thickness (2, 4 and 8 mm).

We noticed as we can sen in figure 1, that this temperature difference (center-surface) starts increasing from the beginning of the thermal shock toward a maximum before diminishing and reaching the thermal equilibrium. Figure 2 represents the maximum temperature difference (center- surface) in function of the thermal shock  $\Delta T$  for the three types of glass. We observe a clear linear relation with an increasing slop as the glass thickness increases.

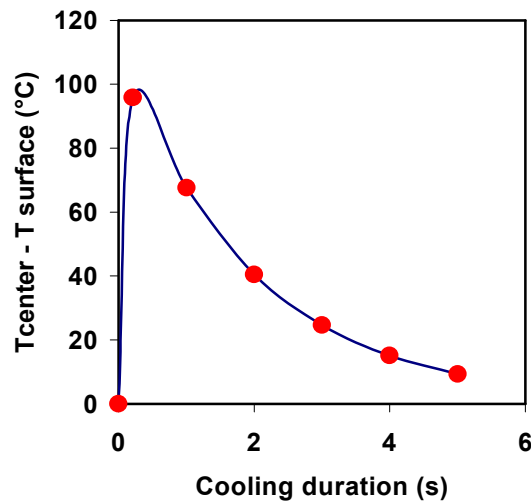


Figure 1: Temperature difference ( $T_c - T_s$ ) in function of the cooling duration for different thermal shock gradients (glass thickness = 4 mm)

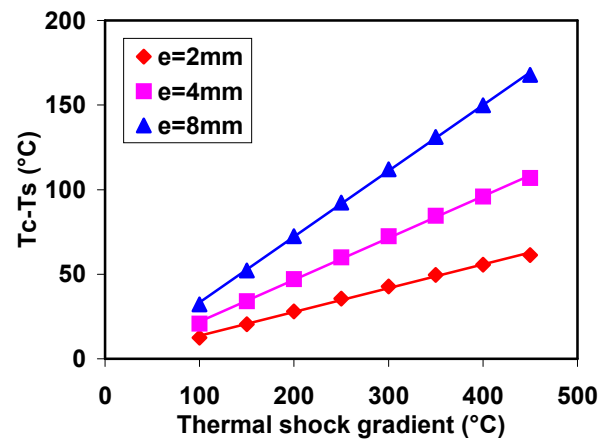


Figure 2: Maximal temperature difference ( $T_c - T_s$ )max in function of the thermal shock gradient for three different thickness of glass

Figure 3 shows the transient stresses evolution in function of the depth for different cooling durations on a glass whose thickness is  $e = 4 \text{ mm}$ . We can see that tensile stresses are maximal on the surface and diminish with depth. They become compressive after a depth corresponding to  $x = e/8$ . The compressive stress at the glass center is about half the maximum tensile stress at the surface. The envelop curve stress shown in figure 3 is obtained to the maximal temperature difference ( $T_c - T_s$ ).

The stress intensity factor was evaluated with the hypothesis of a unidirectional crack of length submitted to the stress profile  $S_{xx}(y, t)$  according to Wu's<sup>7</sup> calculation. In figure 4, we represented the stress intensity factor  $K(a, t)$  evolution with time and flaws size. We notice that the envelope of the curves has a maximum at the time  $t = 0.161$  s. The stress intensity factor  $K(a, t)$  is greater than the critical value  $K_{Ic}$  for that time and a flaw size of  $80 \mu\text{m}$ . This critical flaw size was determined according to linear fracture mechanics rupture. In this conditions, at the end of the thermal shock, a flaw of  $80 \mu\text{m}$  size will reach a final length  $a_f$  about the center of the specimen.

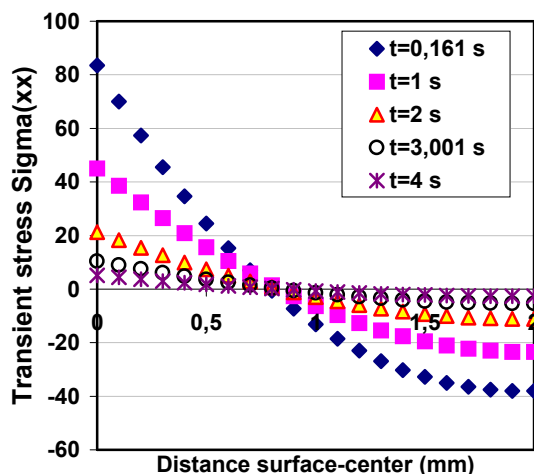


Figure 3: Transient stress  $\sigma_{xx}(y)$  in function of the depth toward the center different temperature ( $\Delta T = 400^\circ\text{C}$ ,  $e = 4$  mm).

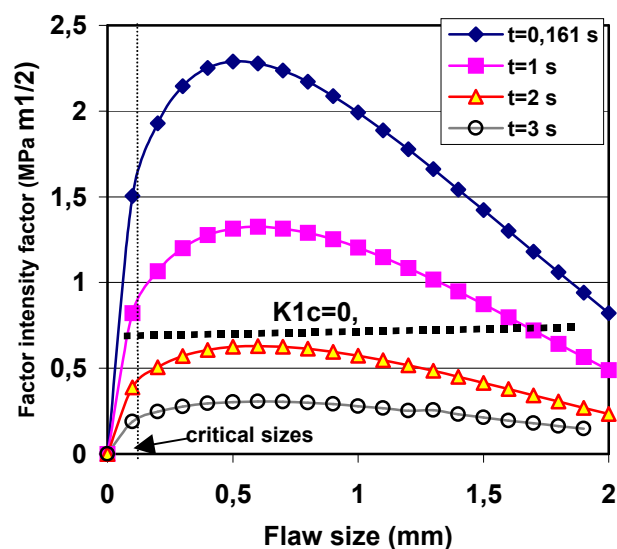


Figure 4: Stress intensity factor versus flaw size

<sup>1</sup> KINGERY, W. D. in *Factors affecting thermal stress resistance of ceramic materials*, Jour. Amer. Ceram. Soc., **38**, (1), (1955) 3–15

<sup>2</sup> HASSELMAN, D. PH. in *Unified theory of thermal shock fracture initiation and crack propagation in brittle ceramics*, Jour. Am. Ceram. Soc., **52**, (11), (1969) 600-604

<sup>3</sup> MANSON, S. S., SMITH, R. W. in *Theory of thermal shock resistance of brittle materials based on Weibull's statistical theory of strength*, Jour. Amer. Ceram. Soc., **38** (1), (1955) 18-27

<sup>4</sup> EVANS, A. G. in *Thermal shock fracture in ceramic materials*, Proc. Br. Ceram. Soc., **25** (1975) 217-35

<sup>5</sup> SCHNEIDER, G. A. in *Thermal shock criteria for ceramics*, Ceram. Inter., **17** (1991) 325-33.

<sup>6</sup> Z. Malou in *Etude de la résistance au choc thermique du verre*, Magister Thesis, Setif university, (1999), P.145.

<sup>7</sup> WU, X.R. - *Application of weight function method for crack analysis in thermal stress field*, Thermal shock and thermal fatigue behavior of advanced ceramics, 8-13 th November, Schlob Ringberg, Germany, G.A. SHNEIDER (eds), Academic publisher, 1992, pp. 1-23